

# Modeling and Tracking Line-Constrained Mechanical Systems

B. Rosenhahn<sup>1</sup>, T. Brox<sup>2</sup>, D. Cremers<sup>3</sup>, and H.-P. Seidel<sup>1</sup>

<sup>1</sup> Max Planck Institute for Computer Science, Stuhlsatzenhausweg 85,  
D-66123 Saarbrücken, Germany  
rosenhahn@mpi-inf.mpg.de

<sup>2</sup> Department of Computer Science, University of Dresden  
01062 Dresden, Germany

<sup>3</sup> Computer Vision Group, University of Bonn  
Römerstr. 164, 53117 Bonn, Germany

**Abstract.** This work deals with modeling and tracking of mechanical systems which are given as kinematic chains with restricted degrees of freedom. Such systems may involve many joints, but due to additional restrictions or mechanical properties the joints depend on each other. So-called closed-chain or parallel manipulators are examples for kinematic chains with additional constraints. Though the degrees of freedom are limited, the complexity of the dynamic equations increases rapidly when studied analytically. In this work, we suggest to avoid this kind of analytic integration of interconnection constraints and instead to model them numerically via soft constraints.

## 1 Introduction

In robotics a kinematic chain represents a set of rigid links which are connected by a set of joints. The term *forward kinematics* of a robot refers to the configuration of an end-effector (the gripper of a robot arm), as a function of joint angles of the robot links. For many systems it is sufficient to deal with prismatic (sliding) or revolute (rotating) joints in a so-called Denavit-Hartenberg parametrization [8]. The term *inverse kinematics* is the opposite problem: given a desired configuration of the end-effector, we are interested in finding the joint angles that achieve this configuration. Despite numerous applications in robotics, the computation of the inverse kinematics is the classical problem statement for motion capturing (MoCap): here the task is to determine the position and orientation as well as the joint angles of a human body from image data. For classical robot manipulators or human beings, the end-effector is (despite physical boundaries) unconstrained, which means that the end-effector can move freely in space. This is also called an open-chain (or serial link) system and many works exist in the fields of robotics and computer vision to compute pose configurations for robots or human beings [4,9,15,14,11,13,18,5].

Besides open-chain systems, a variety of robots is equipped with so-called closed-chain manipulators. A four-bar linkage system is a famous example [16]. A

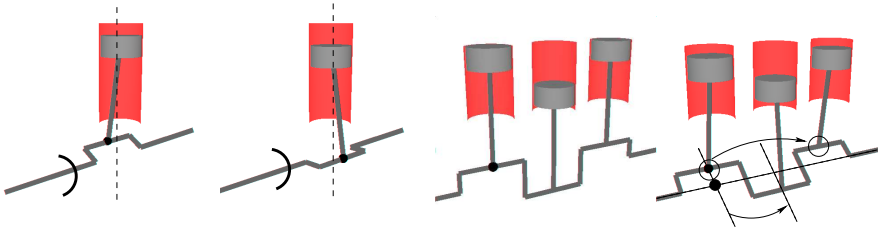


**Fig. 1.** Example frames of a piston (left) or connected pistons as 3 cylinder motor on a crankshaft (right)

generalization of closed-chain manipulators means to constrain parts of a kinematic chain to a limited degree of freedom, thereby reducing the number of degrees of freedom. We call this kind of systems *constrained manipulators*. One example is a piston or connected pistons, see Figure 1, which are constrained to keep a specific orientation due to the cylinder. Though there are three joints involved, just one parameter (e.g. joint angle) is sufficient to determine the remaining angles. This follows from the fact, that the piston can only move along the cylinder by maintaining its orientation. A similar thing happens with the set of pistons on the crankshaft: though  $3 \times 3$  joints are involved, just one single parameter is needed to describe the configuration of the system. Thus, it is important to express the constraint that a piston is only allowed to move up and down inside the cylinder.

Though the number of parameters needed to describe the system configuration is reduced, the complexity of the dynamic equations increases rapidly, since there are constraints between the joint coordinates. For controller design, closed-chain manipulators have been an active topic of research for many years [10,1,12,7,20]. In this work, we do not develop a controller system for active and passive joints. We are rather interested in tracking closed-chain and constrained manipulators from image data. A theoretical work dealing with reduced equations of robotics systems using Lie groups can be found in [17]. Figure 2 shows some examples of constrained manipulators, which we studied in our experiments. For instance, the pantograph type wardrobe model involves eight joints, but since the midpoints of the limbs are connected, the motion is restricted to a translation of the end-effector forwards and backwards. The second example is a rotating crankshaft and piston in a one cylinder engine assembly. Our experiments show that one can successfully capture the single degree of freedom of the piston without explicitly modeling the complex dynamics.

## 2 Twists, Kinematic Chains and Pose Estimation

In this section we recall mathematic foundations needed for modeling the open-chain and constrained manipulators. We further briefly introduce the pose estimation procedure used for the experiments.



**Fig. 2. Top:** Examples for a pantograph type of constrained kinematic chains to lift projectors (left), to adjust a cosmetics mirror (middle), or a wardrobe for children (right). **Bottom:** The second example: a rotating crankshaft and piston in a one cylinder engine assembly. Both types of constrained kinematic chains will be used in the experiments.

### 2.1 Twists

A rigid body motion of a 3D point  $x$  can be expressed in homogeneous coordinates as

$$X' = (x', 1)^T = MX = M(x, 1)^T = \begin{pmatrix} R & t \\ 0_{3 \times 1} & 1 \end{pmatrix} \begin{pmatrix} x \\ 1 \end{pmatrix}. \tag{1}$$

The matrix  $R$  is a rotation matrix,  $R \in SO(3)$  and  $t$  is a translation vector. The set of all matrices of type  $M$  is called the Lie Group  $SE(3)$ . To every Lie group there exists an associated Lie algebra, whose underlying vector space is the tangent space of the Lie group, evaluated at its origin. The Lie algebra associated with  $SE(3)$  is  $se(3) := \{(v, \omega) | v \in \mathbb{R}^3, \omega \in so(3)\}$ , with  $so(3) := \{A \in \mathbb{R}^{3 \times 3} | A = -A^T\}$ . Elements of  $so(3)$  and  $se(3)$  can be written as vectors  $\omega = (\omega_1, \omega_2, \omega_3)^T$ ,  $\xi = (\omega_1, \omega_2, \omega_3, v_1, v_2, v_3)^T$  or matrices

$$\hat{\omega} = \begin{pmatrix} 0 & -\omega_3 & \omega_2 \\ \omega_3 & 0 & -\omega_1 \\ -\omega_2 & \omega_1 & 0 \end{pmatrix}, \hat{\xi} = \begin{pmatrix} \hat{\omega} & v \\ 0_{3 \times 1} & 0 \end{pmatrix}. \tag{2}$$

A twist  $\xi$  can be converted into an element of the Lie group  $M \in SE(3)$  by computation of its exponential form, which can be done efficiently by using the Rodrigues formula [16].

For varying  $\theta$ , the one-parametric Lie-subgroup  $M_\theta = \exp(\theta \hat{\xi})$  yields a screw motion around a fixed axis in space. A degenerate screw (without pitch component) will be used to model revolute joints.

## 2.2 Plücker Lines

3D lines are needed on the one hand for the point-based pose estimation procedure and on the other hand to constrain the constrained manipulators. In this work, we use an implicit representation of a 3D line in its Plücker form [2]. A Plücker line  $L = (n, m)$  is given by a normalized vector  $n$  (the direction of the line) and a vector  $m$ , called the moment, which is defined by  $m := x' \times n$  for a given point  $x'$  on the line. Collinearity of a point  $x$  to a line  $L$  can be expressed by

$$x \in L \Leftrightarrow x \times n - m = 0, \quad (3)$$

and the distance of a point  $x$  to the line  $L$  can easily be computed by  $\|x \times n - m\|$ , see [19] for details.

## 2.3 Kinematic Chains

A kinematic chain is modeled as the consecutive evaluation of exponential functions of twists  $\xi_i$  as done in [3,4]. A point at an end effector, additionally transformed by a rigid body motion is given as

$$X'_i = \exp(\theta \hat{\xi})(\exp(\theta_1 \hat{\xi}_1) \dots \exp(\theta_n \hat{\xi}_n))X_i. \quad (4)$$

In the remainder of this paper we note a pose configuration by the  $(6+n)$ -D vector  $\chi = (\xi, \theta_1, \dots, \theta_n) = (\xi, \Theta)$  consisting of the 6 degrees of freedom for the rigid body motion  $\xi$  and the joint angle vector  $\Theta$ . In our setup, the vector  $\chi$  is unknown and has to be determined from the image data. Furthermore, the angle configuration has to satisfy the additional mechanical constraints of the system.

## 2.4 Registration, Pose Estimation

Assuming an extracted image contour and the silhouette of the projected surface mesh, the closest point correspondences between both contours are used to define a set of corresponding 3D lines and 3D points. Then a 3D point-line based pose estimation algorithm for kinematic chains is applied to minimize the spatial distance between both contours: For point based pose estimation each line is modeled as a 3D Plücker line  $L_i = (n_i, m_i)$  [2]. For pose estimation the reconstructed Plücker lines are combined with the twist representation for rigid motions: Incidence of the transformed 3D point  $X_i$  with the 3D ray  $L_i = (n_i, m_i)$  can be expressed as

$$\pi \left( \exp(\theta \hat{\xi}) X_i \right) \times n_i - m_i = 0. \quad (5)$$

The function  $\pi$  denotes the projection of a homogeneous 4D vector to a 3D vector by neglecting the homogeneous component, which is 1.

For the case of kinematic chains, we exploit the property that joints are expressed as special twists with no pitch of the form  $\theta_j \hat{\xi}_j$ . The sought parameters are the joint angles

$\theta_j$ , whereas  $\hat{\xi}_j$  is known (the location of the rotation axes is part of the model). The constraint equation of an  $i$ th point on a  $j$ th joint reads

$$\pi \left( \exp(\theta \hat{\xi}) \exp(\theta_1 \hat{\xi}_1) \dots \exp(\theta_j \hat{\xi}_j) X_i \right) \times n_i - m_i = 0. \quad (6)$$

To minimize for all correspondences in a least squares sense, we optimize

$$\operatorname{argmin}_{(\xi, \Theta)} \sum_i \left\| \pi \left( \exp(\hat{\xi}) \prod_{j \in \mathcal{J}(x_i)} \exp(\theta_j \hat{\xi}_j) \begin{pmatrix} x_i \\ 1 \end{pmatrix} \right) \times n_i - m_i \right\|_2^2, \quad (7)$$

where  $\mathcal{J}(x_i)$  denotes the set of joints that affect the point  $x_i$ . Linearization of this equation leads to three linear equations with  $6 + j$  unknowns, the six pose parameters and  $j$  joint angles. Collecting enough correspondences yields an over-determined linear system of equations and allows to solve for these unknowns in the least squares sense. Then the Rodrigues formula is applied to reconstruct the group action and the process is iterated until it converges.

## 2.5 The Silhouette Based Tracking System

To represent the silhouette of an object in the image, a level set function  $\Phi \in \Omega \mapsto \mathbb{R}$  is employed. It splits the image domain  $\Omega$  into two regions  $\Omega_1$  and  $\Omega_2$  with  $\Phi(x) > 0$  if  $x \in \Omega_1$  and  $\Phi(x) < 0$  if  $x \in \Omega_2$ . The zero-level line thus marks the boundary between both regions.

For an optimum partitioning, the following energy functional can be minimized. It is an extended version of the Chan-Vese model [6]

$$E(\Phi, p_1, p_2) = - \int_{\Omega} (H(\Phi(x)) \log p_1(I(x)) + (1 - H(\Phi(x))) \log p_2(I(x)) + \nu |\nabla H(\Phi(x))|) dx \quad (8)$$

with a weighting parameter  $\nu > 0$  and  $H(s)$  being a regularized version of the Heaviside (step) function, e.g. the error function. The probability densities  $p_1$  and  $p_2$  measure the fit of an intensity value  $I(x)$  to the corresponding region. We model these densities by local Gaussian distributions [19]. The partitioning and the probability densities  $p_i$  are estimated alternately.

The tracking system in [19] builds upon the previous segmentation model by combining it with the pose tracking problem. To this end, the following coupled energy functional is optimized:

$$E(\Phi, p_1, p_2, \chi) = - \int_{\Omega} (H(\Phi) \log p_1 + (1 - H(\Phi)) \log p_2 + \nu |\nabla H(\Phi)|) dx + \underbrace{\lambda \int_{\Omega} (\Phi - \Phi_0(\chi))^2 dx}_{\text{shape constraint}}. \quad (9)$$

It consists of the above segmentation model and an additional shape constraint that states the pose estimation task. By means of the contour  $\Phi$ , both problems are coupled.

In particular, the projected surface model  $\Phi_0$  acts as a shape prior to support the segmentation [19]. The influence of the shape prior on the segmentation is steered by the parameter  $\lambda = 0.05$ . Due to the nonlinearity of the optimization problem, an iterative, alternating minimization scheme is proposed in [19]: first the pose parameters  $\chi$  are kept constant while the functional is minimized with respect to the partitioning. Then the contour is kept constant while the pose parameters are determined to fit the surface mesh to the silhouettes (Section 2.4).

### 3 Closed-Chain and Constrained Manipulators

To determine the degrees of freedom of a closed-chain manipulator, Grueblers formula can be applied [16]: let  $N$  be the number of links in the mechanism,  $g$  the number of joints, and  $f_i$  the degrees of freedom for the  $i$ th joint. The number of degrees of freedom of the mechanism is

$$F = 6N - \sum_{i=1}^g (6 - f_i) = 6(N - g) + \sum_{i=1}^g f_i. \quad (10)$$

For planar motions, the scalar 6 needs to be replaced by 3.

The key idea of the present work is to use open-chain models and to add constraint equations in the optimization procedure to enforce their configuration as a constrained manipulator. These further constraints will automatically result in equations of rank  $g - F$ , with the degrees of freedom of the mechanism as the remaining unknowns.

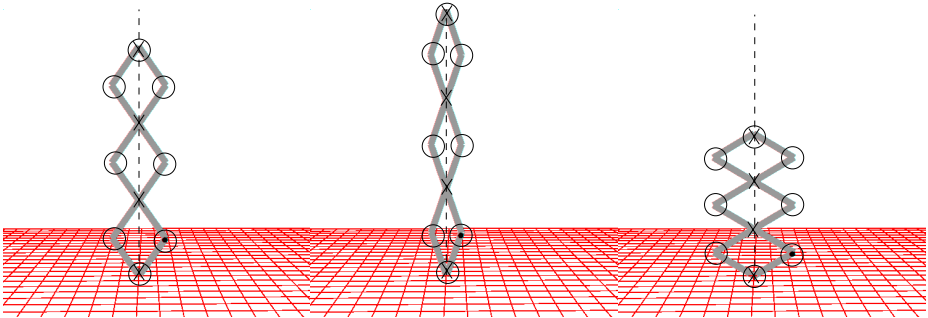


Fig. 3. Example configurations of the wardrobe model from Figure 2 (right)

Take, for instance, Figure 3. Here we have a pantograph assembly with two open-chain manipulators, where mid-points of the links have to be on a straight line and the beginning and end of the two chains have to be incident. The joints are encircled in Figure 3 and the dashed line again shows the geometric invariance of the constrained manipulator which has to be satisfied.

Following (10), the closed-chain system consists of 8 links and 9 joints, yielding  $6(8 - 9) + 8 = -6 + 8 = 2$  degrees of freedom. However, Gruebler's formula only holds when the constraints imposed by the joints are independent. As the midpoints of the

limbs are partially connected, here we have only one degree of freedom resulting in a translation of the end-effector forwards and backwards.

We define  $L_m = (n_m, m_m)$  as the (dashed) midline of the constrained system, see Figure 3 and collect a set of points  $p_i$  on the model which have to be incident with  $L_m$ ,

$$\forall i : p_i \times n_m - m_m = 0. \tag{11}$$

The model in Figure 3 contains 8 joints, each with one degree of freedom and we gain 6 collinearity equations for the system. If these equations are collected and ordered in a system of equations, we get a system of rank 6, which means at least one additional point correspondence is needed to determine the configurations of the constrained system, though in this case eight joints are involved.

The same is possible for the examples in Figure 1 (left): in principle the piston is an open-chain manipulator with the property that the piston has to move along a straight line (the dashed line in the Figure). Though 3 joints are involved only one 3D point is sufficient to determine the configuration of the system. Figure 1 shows on the right hand side a set of connected pistons. Here again, the fact that the pistons are required to move along a line can be applied to constrain one of the joints. The first piston is again determined from the moving point (shown as black dot). The second and third piston can be determined from the configuration of the first one. In the animations of Figures 1 and 3, only the black point is used to determine the joint configuration of the manipulators.

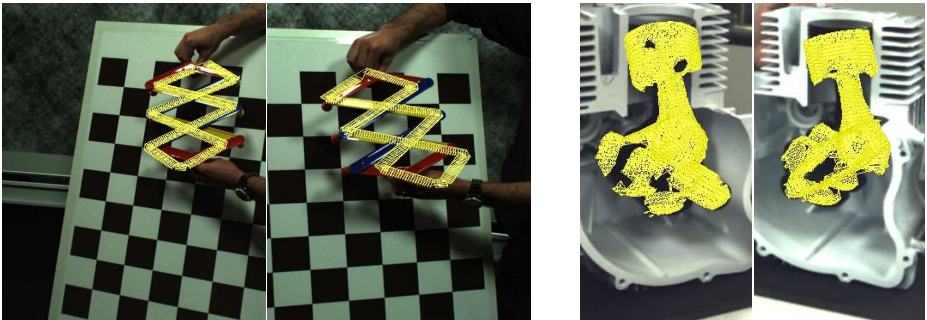


**Fig. 4.** Pose results of the non-constrained models: the first model tends to break apart and the top of the cylinder in the second model is tilted. Overall, the outcome is less stable.

We therefore use a point-line constraint to model the geometric properties of the constrained manipulator. It is exactly the same constraint we use for optimizing the pose parameters, which means we can directly integrate the equations in the optimization procedure of our tracking system by collecting equations to minimize

$$\operatorname{argmin}_{(\xi, \theta)} \sum_i \left\| \pi \left( \exp(\hat{\xi}) \prod_{j \in \mathcal{J}(p_i)} \exp(\theta_j \hat{\xi}_j) \begin{pmatrix} p_i \\ 1 \end{pmatrix} \right) \times n_m - m_m \right\|^2. \tag{12}$$

Note, that the unknowns are the same as for Equation (7), the unknown pose parameters. Only the line  $L_m = (n_m, m_m)$  is not due to a reconstructed image point, but stems from the object model. Since we use a point-line constraint to restrict the movement of the manipulators, we call them *line-constrained mechanical systems*.

The matrix of gathered linear equations is attached to the one presented in Section 2.4. Its effect is to regularize the equations and to constrain the solution to a desired subspace of possible joint configurations. The structure of the generated linear system is  $A\chi = b$ , with two attached parts, generated from equation (7) and (12) in the same unknowns  $\chi$ .

Since this is a soft constraint for the constrained manipulator configuration that is integrated in a least squares sense, it can happen that the constraint is not fully satisfied due to errors in the point correspondences collected from the image data. This effect can be reduced by multiplying the constraint equations by a strong weight. In our experiments, the pose of the open chain system had a deviation of less than 0.01 degrees compared to an explicitly modeled constrained system, see Figure 6. For most tracking applications, this accuracy is sufficient.

## 4 Experiments

In this section we present experimental results of constrained manipulators we tracked in stereo setups.

For comparison to our proposed method, Figure 4 shows pose results of the models when the additional constraints are neglected. This comes down to an unconstrained

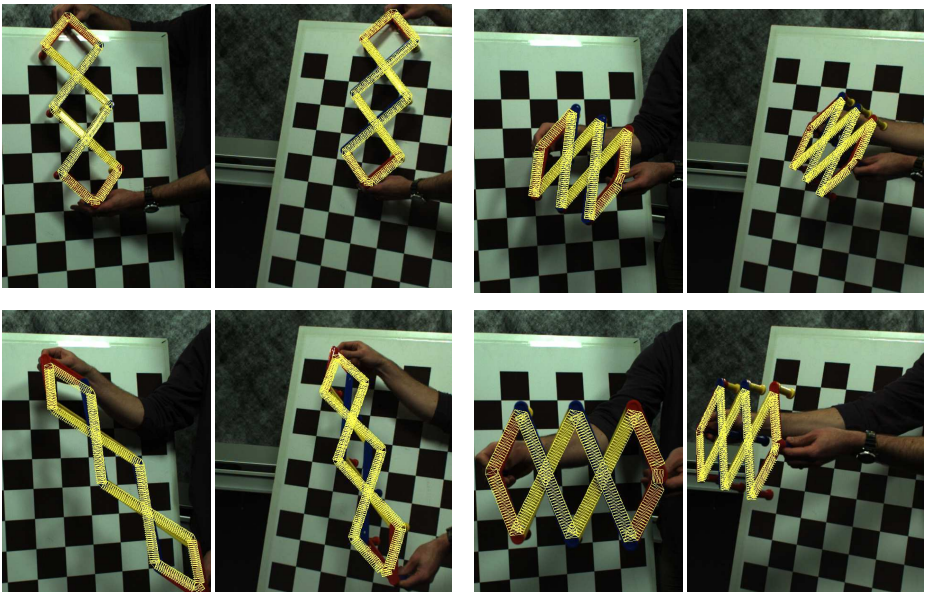
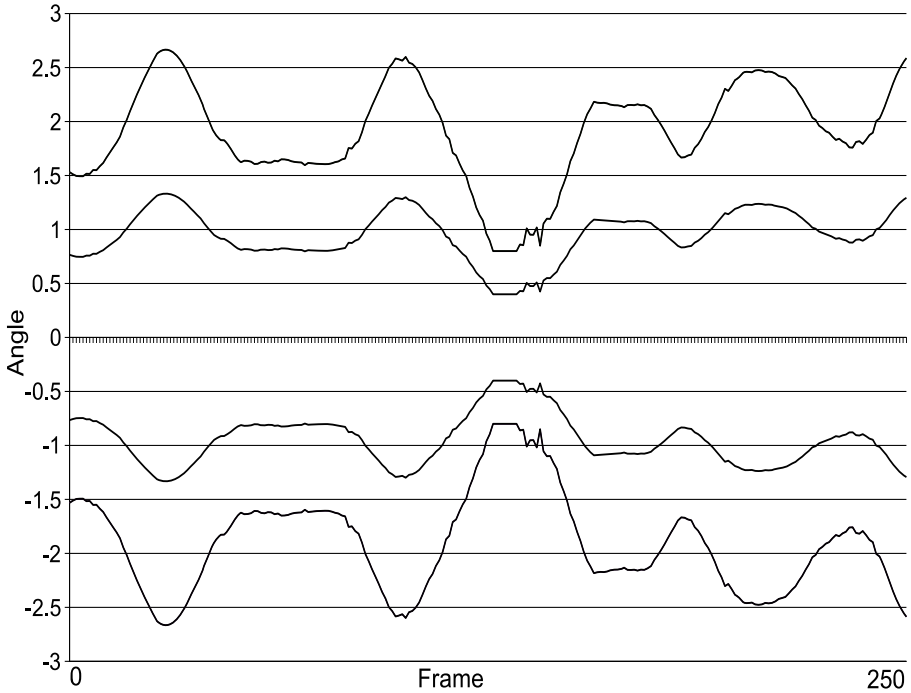


Fig. 5. Pose results of the wardrobe model moving freely in a cluttered scene

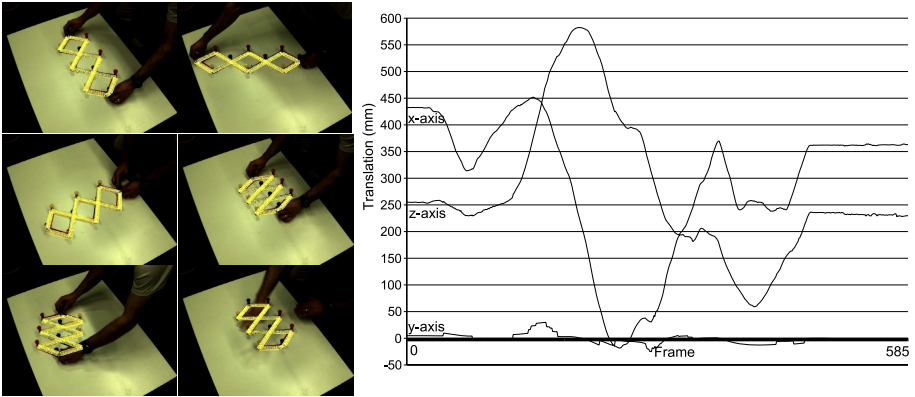


**Fig. 6.** Angles of the linkage system

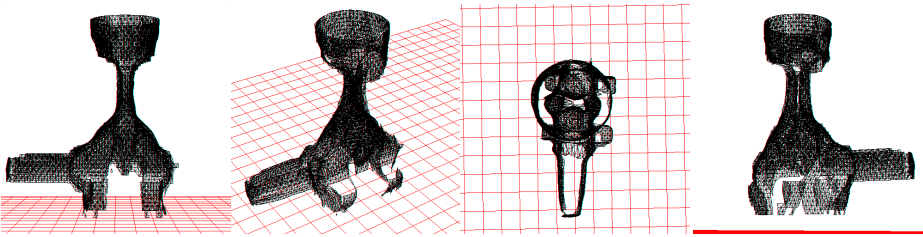
open chain model with more degrees of freedom than actually allowed. The first model tends to break apart and the top of the piston in the second model is tilted. Overall, the tracking is erroneous and unreliable. Figure 5 shows four examples of the first test sequence (250 frames). Here the object model moves freely in 3D space. The manual interaction visible in the scene (the arms behind the object model) rules out background subtraction methods for this tracking task. The algorithm successfully tracks the object and maintains its intrinsic constraints.

Figure 6 shows angles of the closed-chain manipulator during tracking. The result clearly reflects the inherent mechanical constraints of the closed chain. It also reveals that in the end only one parameter is needed to determine the configuration of the system. The smooth curves indicate a stable tracking.

In the second set-up, see Figure 7, we decided on a controlled environment (non-cluttered back ground) and restricted movements: The object is only moved along the ground plane while it is stretched and squeezed. Figure 7 shows in the left six example frames of a 585 frame stereo-sequence and in the right the translation vectors in millimeters. The deviation of the y-axis varies up to 3cm and indicates a reasonable stable result. Note, that during the last 100 frames, the model was kept still, while a hand was moved in front of the object, yielding to partial occlusions. The nearly constant



**Fig. 7.** Left, Pose results: During tracking, the model is squeezed and stretched while moving it along a 3D plane. In the last 100 frames, the model is kept still and a hand moving in front of the model is causing partial occlusions. Right: The translation vectors along the  $x$ ,  $y$  and  $z$ -axes in millimeter. The deviation along the  $y$ -axis varies up to 3cm which indicates a reasonable stable result.



**Fig. 8.** Laser scan of a piston. The scan contains several holes and missing parts, which are taken as an additional challenge for tracking.

translation values indicate a reasonably stable pose result. The average deviation from the ground plane was 6 mm.

A motor from a mower was used for the second experimental setup. It was modified by milling off one side of the motor block. Then the motor was painted white and the piston, connecting rod and crankshaft painted black, see Figure 2 (bottom). The piston, the connecting rod and crankshaft was then scanned with a laser scanner, see Figure 8, and joints were added to the mesh model. The laser scan contains some holes and artefacts, which have been regarded as an additional challenge for tracking.

Figure 9 shows some pose results of a sequence (730 frames) in which the piston is rotating several times around the crankshaft. The artefacts of the laser scan are clearly visible. They hinder the correct segmentation, since the shape model does not fully reflect the appearance of the object. Nonetheless, due to the stereo information of both

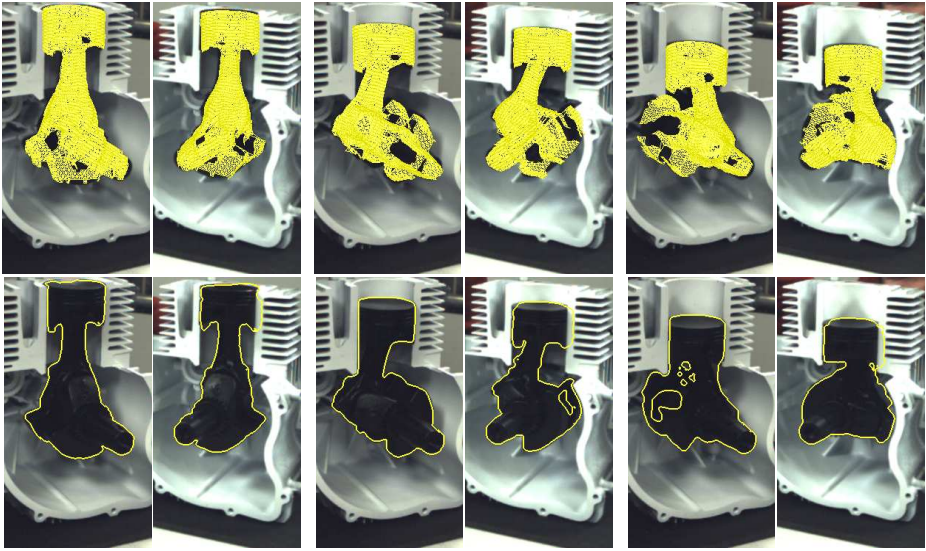


**Fig. 9.** Pose and segmentation results during tracking the piston (images are cropped). The artefacts from the laser scanner are clearly visible. Nonetheless, the tracking is successful.

cameras and the additional implicit constraint that the piston can only move upwards and downwards, the object is tracked successfully. Figure 10 shows the sine-value of the angles during tracking the piston model. Two aspects can be observed: just one parameter is optimized, so that the three angles are correlated and their dependency is non-linear. An explicit modeling of the constrained kinematic system would require higher order trigonometric functions, which are avoided here.

## 5 Summary

In this paper we presented an extension of a tracking system that, so far, only allowed for open-chain manipulators such as human beings or robot arms. The extended system allows to track constrained kinematic chains. This includes models which can involve many joints with coupled degrees of freedom. The analytic examination of such constrained kinematic chains leads to rapidly increasing complexity of the dynamic equations. To deal with the inherent restrictions, we suggest to use open chain systems and to add model constraints such as a couple of points that have to be incident with a given line. Implicitly, these model constraints ensure a reduced rank of the system, so the minimal number of point correspondences is sufficient to compute the configuration of the whole system. At the same time, the model constraints ensure that the dynamical system behaves like a closed-chain system. The experiments show that the developed system works reliably, even in the presence of cluttered and varying background in the scene.

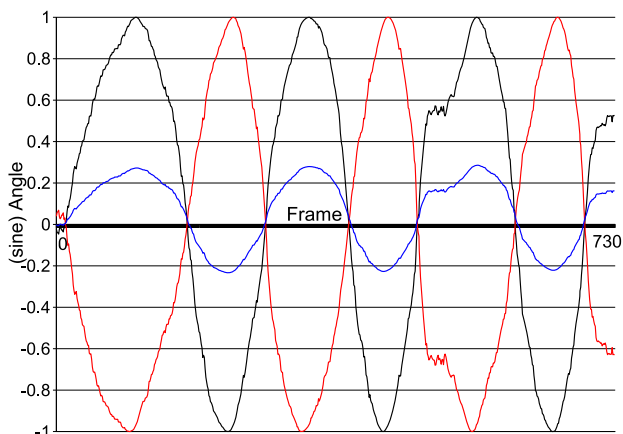


**Fig. 10.** The sine-values of angles of the piston sequence

## Acknowledgments

This work has been supported by the Max-Planck Center for Visual Computing and Communication. We would like to thank Christian Fuchs and Axel Köppel from the Max-Planck Institute for Computer Science for their help with the one cylinder engine.

## References

1. Bicchi, A., Prattichizzo, D.: On some structural properties of general manipulation systems. In: Astolfi, A., et al. (eds.) *Modelling and Control of Mechanical Systems*, pp. 187–202. Imperial College Press, London, U.K (1997)
2. Blaschke, W.: *Kinematik und Quaternionen*, Mathematische Monographien, Deutscher Verlag der Wissenschaften, vol. 4 (1960)
3. Bregler, C., Malik, J.: Tracking people with twists and exponential maps. In: *Proc. Computer Vision and Pattern Recognition*, Santa Barbara, California, pp. 8–15 (1998)
4. Bregler, C., Malik, J., Pullen, K.: Twist based acquisition and tracking of animal and human kinetics. *International Journal of Computer Vision* 56(3), 179–194 (2004)
5. Carranza, J., et al.: Free-viewpoint video of human actors. In: *Proc. SIGGRAPH 2003*, pp. 569–577 (2003)
6. Chan, T., Vese, L.: Active contours without edges. *IEEE Transactions on Image Processing* 10(2), 266–277 (2001)
7. Cheng, H., Yiu, Y.: Dynamics and control of redundantly actuated parallel manipulators. *Trans. on Mechatronics* 8(4), 483–491 (2003)
8. Denavit, J., Hartenberg, R.S.: A kinematic notation for lower-pair mechanisms based on matrices. *ASME Journal of Applied Mechanics* 22, 215–221 (1955)
9. Fua, P., Plänkers, R., Thalmann, D.: Tracking and modeling people in video sequences. *Computer Vision and Image Understanding* 81(3), 285–302 (2001)
10. Gao, X., Qu, Z.: On the robust control of two manipulators holding a rigid object. *Intelligent and Robotic Systems* 8, 107–119 (1992)

11. Gavrilu, D.M.: The visual analysis of human movement: A survey. *Computer Vision and Image Understanding* 73(1), 82–92 (1999)
12. Kim, D., Kang, J., Lee, K.: Robust tracking control design for a 6 dof parallel manipulator. *Journal of Robotics Systems* 17(10), 527–547 (2000)
13. Mikic, I., et al.: Human body model acquisition and tracking using voxel data. *International Journal of Computer Vision* 53(3), 199–223 (2003)
14. Moeslund, T.B., Hilton, A., Krüger, V.: A survey of advances in vision-based human motion capture and analysis. *Computer Vision and Image Understanding* 104(2), 90–126 (2006)
15. Moeslund, T.B., Granum, E.: A survey of computer vision based human motion capture. *Computer Vision and Image Understanding* 81(3), 231–268 (2001)
16. Murray, R.M., Li, Z., Sastry, S.S.: *Mathematical Introduction to Robotic Manipulation*. CRC Press, Baton Rouge (1994)
17. Ostrowski, J.: Computing reduced equations for robotic systems with constraints and symmetries. *Trans. on Robotics and Automation* 15(1), 111–123 (1999)
18. Rosenhahn, B.: Pose estimation revisited. Technical Report TR-0308, PhD-thesis, Institute of Computer Science, University of Kiel, Germany (October 2003), <http://www.ks.informatik.uni-kiel.de>
19. Rosenhahn, B., Brox, T., Weickert, J.: Three-dimensional shape knowledge for joint image segmentation and pose tracking. *International Journal of Computer Vision* 73(3), 243–262 (2007)
20. Zweiri, Y., Senevirante, L., Althoefer, K.: Modelling of closed-chain manipulators on an excavator vehicle. *Mathematical and Computer Modeling of Dynamical Systems* 12(4), 329–345 (2003)